

Improved dynamics of a tunnelling-injection quantum-dot laser under optical feedback

Faezeh Asadi, Abbas Zarifkar

Abstract. We report an investigation of the optical feedback effect on the dynamics of a tunnelling-injection quantum dot (TI QD) semiconductor laser. Assuming the external cavity to be short and using a small signal analysis, the modulation response of a TI QD laser is calculated under optical feedback conditions. The impact of the tunnelling probability, bias-current density, feedback ratio, external cavity length and linewidth enhancement factor on the modulation response of a TI laser is studied. With the optical feedback taken into account, the modulation responses of conventional and TI QD lasers are compared. The obtained results demonstrate that at an appropriate feedback ratio and external cavity length, the laser bandwidth and its relaxation frequency can be improved.

Keywords: modulation response, quantum dot laser, tunnelling injection.

1. Introduction

Quantum dot (QD) lasers have attracted much attention in the recent decade due to their suitable characteristics which originate from a three dimensional confinement of carriers in the active region and discrete nature of their density of states. The main advantages of QD lasers are the low threshold current [1,2], temperature insensitivity [3–6], high bandwidth [7,8] and low chirp [9,10]. However, one of the main drawbacks of QD lasers is the hot-carrier problem which limits the modulation rate of lasers [11]. In order to alleviate problems related to hot carriers in the active region, a tunnelling-injection quantum-dot (TI QD) laser was proposed [11]. In TI QD lasers, carriers tunnel from a reservoir directly into the ground state or lasing state. Thus, by injecting carriers into the ground state, some characteristics such as the laser bandwidth are improved and several deleterious effects such as the frequency chirp are reduced [11]. In optical fibre telecommunication, the laser receives an optical feedback from a fibre pigtail tip or optical fibre connectors. Even a small backreflection of light into a diode laser module can be considered as a source of instability in many situations. On the other hand, the optical feedback can enhance the modulation characteristics and decrease the intensity noise [12]. In 2012, Otto et al. [13] investigated the first three external cavity modes using a bifurcation diagram of QD lasers under optical feedback. By calculating

the first Hopf bifurcation, they concluded that the critical feedback level is proportional to the damping factor of the oscillation frequency while it is inversely determined by the linewidth enhancement factor [13]. The influence of external optical feedback on the linewidth enhancement factor of semiconductor lasers was studied by Yu and Xi in 2013 [14], who showed that there is a strong correlation between the external optical feedback and the linewidth enhancement factor. Virte et al. [15] demonstrated that an increase in the optical feedback rate leads to lasing from the excited state (ES) in a single mode, while under the threshold condition, QD lasers emit simultaneously from the ground state (GS) and ES. The frequency chirp of self-injected QD lasers has been investigated in 2013 by Wang et al. [16]. In their calculations they found that the chirp-to-power ratio (CPR) is sensitive to optical feedback conditions at any modulation frequencies. Also, they showed that for short external cavity lengths, the modulation properties of the laser can be improved.

In this paper, we consider for the first time TI QD lasers under external optical feedback and show the impact of different parameters such as the feedback ratio, tunnelling probability, current density and linewidth enhancement factor on the modulation response of these lasers.

2. Theoretical analysis

The 1.3- μm TI QD laser heterostructure, the dynamics of carriers and photons in the active region and the basic scheme of the TI laser operating under external optical feedback are shown in Fig. 1. The active region contains five InGaAs QD layers within GaAs barriers, as well as an AlGaAs barrier layer and an InGaAs quantum-well (QW) layer. The laser uses only one QD ensemble of equal size and shape, which includes two energy levels corresponding to the ground state and the excited state.

A group of carriers (Fig. 1b) that are injected into the separate confinement layer (SCL) tunnel into the GS (with the tunnelling factor ε_t) and the other carriers pass the barrier and enter the wetting layer (WL) and finally relax to the GS through the ES. We use the following system of rate equations to describe the dynamics of carriers, photons [17] and the phase of the optical beam in the TI QD laser under optical feedback [12]:

$$\frac{\partial N_s}{\partial t} = \frac{J}{qL_s} - \varepsilon_t \frac{N_s}{\tau_t} (1-f) - (1-\varepsilon_t) \frac{N_s}{\tau_d}, \quad (1a)$$

$$\frac{\partial N_w}{\partial t} = (1-\varepsilon_t) \frac{N_s L_s}{\tau_t L_w} - \frac{N_w}{\tau_{w2}} (1-h) + \frac{N_w h}{\tau_{2w}} - \frac{N_w}{\tau_{wr}}, \quad (1b)$$

Faezeh Asadi, Abbas Zarifkar Department of Communications and Electronics, School of Electrical and Computer Engineering, Shiraz University, Shiraz, Iran; e-mail: zarifkar@shirazu.ac.ir

Received 12 July 2016; revision received 31 August 2016
Kvantovaya Elektronika 46 (10) 883–887 (2016)
Submitted in English

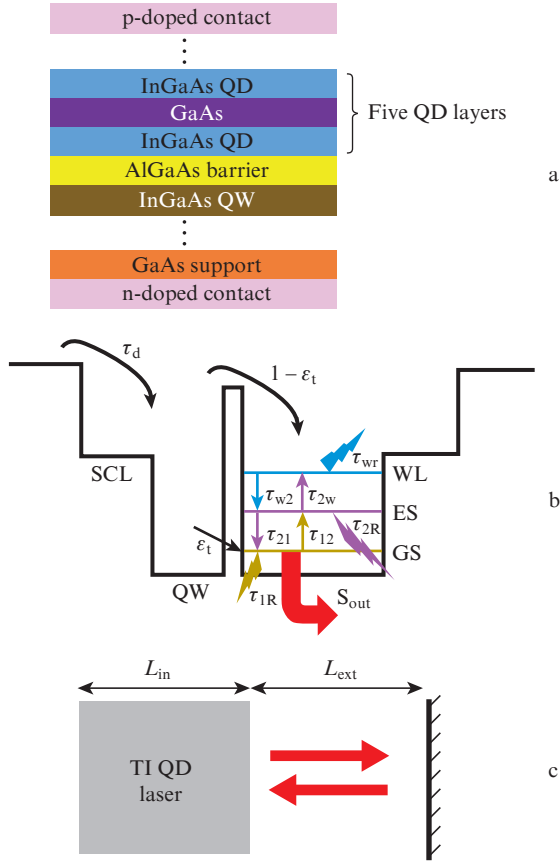


Figure 1. (a) Schematics of a TI QD laser ($\lambda = 1.3 \mu\text{m}$), (b) dynamics of carriers and photons in the active region of the laser [17] and (c) TI QD laser under external optical feedback; L_{in} and L_{ext} are the lengths of the laser cavity and external cavity with optical feedback; S_{out} is the output intensity; other notations are given in the text.

$$\frac{\partial(N_Q h)}{\partial t} = (1-h) \frac{N_w}{\tau_{w2}} - \frac{N_w h}{\tau_{2w}} - \frac{N_Q h}{\tau_{21}} (1-f) + \frac{N_Q f}{\tau_{12}} (1-h) - \frac{N_Q h}{\tau_{2R}}, \quad (1c)$$

$$\frac{\partial(N_Q f)}{\partial t} = \frac{N_s L_s \varepsilon_t}{\tau_t L_w} (1-f) - \frac{N_Q}{\tau_{1R}} f^2 - V_g g_1 (2f-1) S_1 + \frac{N_Q h}{\tau_{21}} (1-f) - \frac{N_Q f}{\tau_{12}} (1-h), \quad (1d)$$

$$\frac{\partial S_1}{\partial t} = \Gamma V_g g_1 (2f-1) S_1 - \frac{S_1}{\tau_p} + \frac{2\beta N_Q f}{\tau_{1R}} + \frac{2K_C}{\tau_{\text{in}}} \sqrt{S_1(t) S_1(t-t_{\text{ext}})} \cos(\Delta\phi), \quad (1e)$$

$$\frac{\partial \phi}{\partial t} = \frac{\alpha_H}{2} \left[\Gamma V_g g_1 (2f-1) - \frac{1}{\tau_p} \right] - \frac{K_C}{\tau_{\text{in}}} \sqrt{S_1(t-t_{\text{ext}})/S_1(t)} \sin(\Delta\phi). \quad (1f)$$

Here, N_s and N_w are the carrier densities in the SCL and WL, respectively; N_Q is the volume density of the QD; q is the electron charge; S_1 is the photon density; J is the current density; L_s and L_w are the SCL and WL thicknesses; ε_t is the tunnelling probability, which takes a constant value between 0 and 1; τ_t and τ_d are the tunnelling and diffusion lifetimes in the SCL;

f and h are the electron occupation probabilities in the GS and ES; τ_{w2} and τ_{2w} are the electron relaxation times from the WL to the ES and the escape time of electrons from the ES to the WL; τ_{wr} , τ_{2R} and τ_{1R} are the spontaneous emission lifetime to the WL, ES and GS; g_1 is the maximum differential gain of the GS; V_g is the group velocity; Γ is the confinement factor; τ_p is the photon lifetime; and β is the spontaneous emission factor. The descriptions and values of all the parameters used in this model are below [12, 17].

Tunnelling probability	0.95
QD volume density/ m^{-3}	2.5×10^{23}
Group velocity/ m s^{-1}	8.57×10^7
Spontaneous emission factor	10^{-5}
Electron relaxation time from the WL to the ES τ_{w2} /s	10^{-12}
Spontaneous radiative lifetime at the GS τ_{1R} /s	0.7×10^{-9}
Spontaneous radiative lifetime at the ES τ_{2R} /s	0.7×10^{-9}
Spontaneous radiative lifetime at the WL τ_{wr} /s	0.7×10^{-9}
Electron relaxation time from the ES to GS τ_{21} **/s	8×10^{-12}
Diffusion lifetime into the SCL/s	0.3×10^{-12}
Energy level difference between the WL and ES ΔE_{w2} /meV	40
Energy level difference between the ES and GS ΔE_{21} /meV	50
Photon lifetime/s	12×10^{-12}
Modal gain $\Gamma g_1/\text{m}^{-1}$	1100
SCL thickness/m	10^{-9}
WL thickness/m	10^{-9}
Facet reflectivity R_1	0.33
External cavity length/cm	0.35
Reflective index in the external cavity n_{ext}	1.5
Linewidth enhancement factor α_H	1

In equations (1e) and (1f), the strength of the optical feedback is defined as [12]:

$$K_C = \frac{1-R_1}{\sqrt{R_1}} \sqrt{F_{\text{ext}}}, \quad (2)$$

where R_1 is the laser facet reflectivity and F_{ext} is the feedback ratio, which is defined as the ratio of the returned power to the emitted one. In the last two rate equations

$$\Delta\phi = \omega_0 \tau_{\text{ext}} + \phi(t) - \phi(t-t_{\text{ext}}) \quad (3)$$

is the phase variation of the field [12], where ω_0 is the centre frequency of photons in the cavity, and the round trip time of photons in the laser cavity, τ_{in} , and the external cavity, t_{ext} , are expressed as [18]

$$t_{\text{ext}} = 2L_{\text{ext}} n_{\text{ext}}/c, \quad (4)$$

$$\tau_{\text{in}} = 2L_{\text{in}}/V_g. \quad (5)$$

To calculate the modulation response of a TI QD laser, small signals are assumed time dependent for carriers and photon densities

$$N_s(t) = N_{sQ} + \delta N_s \exp(i\omega t), \quad (6a)$$

$$N_w(t) = N_{wQ} + \delta N_w \exp(i\omega t), \quad (6b)$$

* The electron escape time from the ES to the WL is $\tau_{2w} = \tau_{w2} \exp(\Delta E_{w2}/k_B T)$.

** The electron escape time from the GS to the ES is $\tau_{12} = \tau_{21} \exp(\Delta E_{21}/k_B T)$.

$$h(t) = h_Q + \delta h \exp(i\omega t), \quad (6c)$$

$$f(t) = f_Q + \delta f \exp(i\omega t), \quad (6d)$$

$$S_1(t) = S_{1Q} + \delta S_1 \exp(i\omega t), \quad (6e)$$

$$\phi(t) = \phi_{Qt} + \delta \phi \exp(i\omega t). \quad (6f)$$

For the phase term, we have the following relations [12]

$$\cos(\Delta\phi) = P[1 + \alpha_H \delta \phi \exp(i\omega t)(1 - \exp(-i\omega t_{\text{ext}}))], \quad (7)$$

$$\sin(\Delta\phi) = P[-\alpha_H + \delta \phi \exp(i\omega t)(1 - \exp(-i\omega t_{\text{ext}}))], \quad (8)$$

$$P = (1 + \alpha_H^2)^{-1/2}. \quad (9)$$

We can calculate the steady-state values (N_{sQ} , N_{wQ} , f_Q , h_Q , S_{1Q}) by solving the system of rate equations (6) using the Runge–Kutta method. After neglecting the quadratic and higher-power small-signal terms in the rate equations, we can obtain the linearised equations:

$$\left(i\omega - \frac{f_Q \varepsilon_t}{\tau_t} + \frac{\varepsilon_t}{\tau_t} + \frac{1 - \varepsilon_t}{\tau_d}\right) \delta N_s - \frac{\varepsilon_t N_{sQ}}{\tau_t} \delta f = \frac{\delta J}{qL_s}, \quad (10a)$$

$$-\left[\frac{(1 - \varepsilon_t)L_s}{\tau_t L_w}\right] \delta N_s + \left(i\omega - \frac{h_Q - 1}{\tau_{w2}}\right) \delta N_w - \frac{N_{wQ}}{\tau_{w2}} \delta h = 0, \quad (10b)$$

$$-\left(\frac{1 - h_Q}{\tau_{w2} N_Q} - \frac{h_Q}{\tau_{2w} N_Q}\right) \delta N_w + \left(i\omega + \frac{N_{wQ}}{\tau_{w2} N_Q} + \frac{N_{wQ}}{\tau_{2w} N_Q} - \frac{f_Q - 1}{\tau_{21}} + \frac{f_Q}{\tau_{21}} + \frac{1}{\tau_{2R}}\right) \delta h - \left(\frac{h_Q}{\tau_{21}} + \frac{1 - h_Q}{\tau_{12}}\right) \delta f = 0, \quad (10c)$$

$$-\left[\frac{L_s \varepsilon_t (1 - f_Q)}{L_w \tau_t N_Q}\right] \delta N_s - \left(\frac{1 - f_Q}{\tau_{21}} + \frac{f_Q}{\tau_{12}}\right) \delta h + \left(i\omega + \frac{N_{sQ} L_s \varepsilon_t}{L_w \tau_t N_Q} + \frac{2}{N_Q} V_g g_1 S_{1Q} + \frac{h_Q}{\tau_{21}} \frac{h_Q - 1}{\tau_{12}} + \frac{2f_Q}{\tau_{1R}}\right) \delta f - \left[\frac{V_g g_1 (1 - 2f_Q)}{N_Q}\right] \delta S_1 = 0, \quad (10d)$$

$$-\left(2\Gamma V_g g_1 S_{1Q} + \frac{2\beta N_Q}{\tau_{1R}}\right) \delta f + \left[i\omega - \frac{PK_C}{\tau_{in}} (1 + \exp(-i\omega t_{\text{ext}}))\right] \delta S_1 - \left[\frac{2PS_{1Q} \alpha_H K_C}{\tau_{in}} (1 - \exp(-i\omega t_{\text{ext}}))\right] \delta \phi = 0, \quad (10e)$$

$$-(\alpha_H \Gamma V_g g_1) \delta f + \left[\frac{PK_C \alpha_H}{2\tau_{in} S_{1Q}} (1 - \exp(-i\omega t_{\text{ext}}))\right] \delta S_1 + \left[i\omega + \frac{K_C P}{\tau_{in}} (1 - \exp(-i\omega t_{\text{ext}}))\right] \delta \phi = 0. \quad (10f)$$

After the Fourier transform of the small-signal rate equations, we can write these equations as linear matrix equations

$$\sum_{l=1}^6 [b_{ml}(\omega)]_{6 \times 6} [\delta X(\omega)]_{6 \times 1} = \left[\frac{\delta J(\omega)}{qL_s}\right]_{6 \times 1}, \quad (11)$$

$$X = N_s, N_w, h, f, S_1, \phi, \quad (11)$$

$$H(\omega) = \frac{\text{Det}[b'_{ml}]_{6 \times 6}}{\text{Det}[b_{ml}]_{6 \times 6}}. \quad (12)$$

The square matrix $[b_{ml}]_{6 \times 6}$ is formed by the coefficients of the system of equations (10a)–(10f). According to Eqn (12), for calculating the modulation response of a TI QD laser we should evaluate the value of $\text{Det}[b'_{ml}]_{6 \times 6}$, which is the determinant of the matrix coefficients where its fifth column is replaced by a vector matrix $[K_m]_{6 \times 1}$. This vector matrix has zero elements except its m_{th} element which is equal to unity. By solving the above equation, various quantities of a TI QD laser can be calculated. Based on these calculations, we will discuss in the following section the effects of different parameters, such as the tunnelling probability and the feedback ratio, on the modulation response of a TI QD laser.

3. Results and discussion

To study the modulation response and dynamics of a TI QD laser under external optical feedback, firstly, we have to determine the steady-state properties of the device by solving the rate equations at constant injection currents. The carrier occupation in the GS and the dependence of the photon density on the injection current density without optical feedback is shown in Fig. 2. The threshold current density J_{th} for the emission from the GS is $0.4 \times 10^5 \text{ A m}^{-2}$.

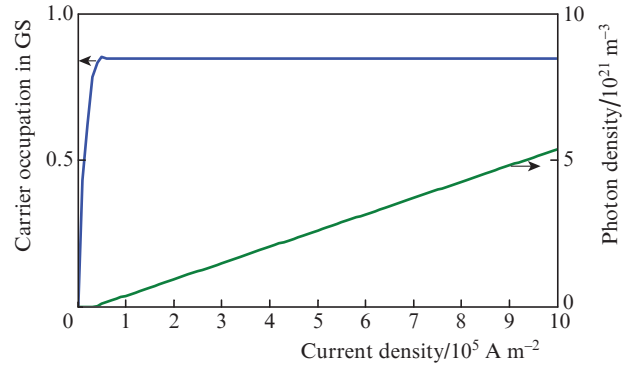


Figure 2. Dependence of the carrier occupation and photon density on the current density for a TI QD laser.

The modulation response of a TI QD laser is calculated for three different values of the feedback ratio (Fig. 3). Calculations imply that by increasing the feedback level, the

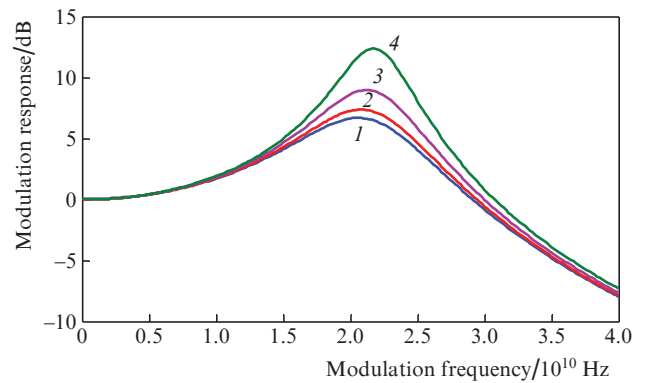


Figure 3. Effect of the feedback ratio on the modulation response of a TI laser in the absence of optical feedback (1) and at $F_{\text{ext}} =$ (2) 10^{-4} , (3) 10^{-3} and (4) 5×10^{-3} .

modulation bandwidth of the TI QD laser increases. In the best case in our simulations at $F_{\text{ext}} = 5 \times 10^{-3}$, the modulation bandwidth enhances to 33.92 GHz, in agreement with the recent theoretical research on the modulation response of QD lasers [12].

Figure 4 shows the effect of the external cavity length on the modulation response of a TI QD laser for a feedback level $F_{\text{ext}} = 10^{-3}$ and $J = 3J_{\text{th}}$. One can see that the external cavity length plays a significant role in the formation of the reflected wave phase ωt_{ext} and consequently the modulation bandwidth of the TI QD laser.

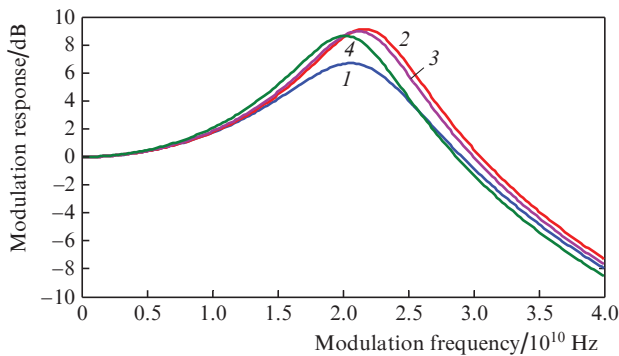


Figure 4. Effect of the external cavity length on the modulation response for $J = 3J_{\text{th}}$ in the absence of optical feedback (1) and $F_{\text{ext}} = 10^{-3}$, $L_{\text{ext}} =$ (2) 0.20, (3) 0.35 and (4) 0.45 cm.

To investigate the effects of the linewidth enhancement factor (LEF) on the modulation response of the TI QD laser, we have plotted the modulation response of the TI QD laser for three different values of the LEF (Fig. 5). One can see that the 3-dB modulation bandwidth of the TI QD laser increases with increasing LEF. The maximum modulation bandwidth is achieved at $\text{LEF} = 5$ and the resonance frequency F_r in this case reaches to 30 GHz.

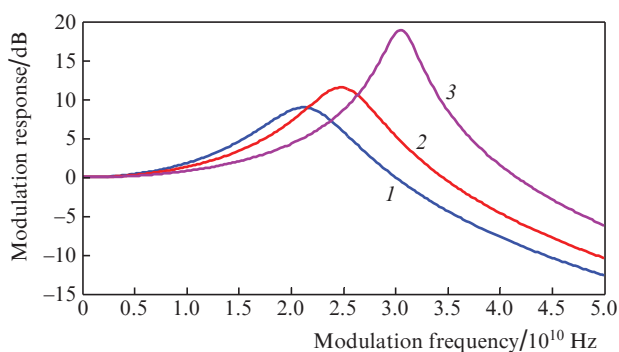


Figure 5. Modulation response of the TI QD laser at $\text{LEF} =$ (1) 1, (2) 3 and (3) 5.

Figure 6 shows the modulation response of the TI QD laser at three different injection currents. The calculation results indicate that the relaxation frequency and damping factor increase with increasing injection current. Therefore, at the injection current of about $4J_{\text{th}}$, the modulation bandwidth reaches the maximum value of ~ 39 GHz.

As follows from the rate equations, the value of tunnelling probability also significantly affects the modulation response

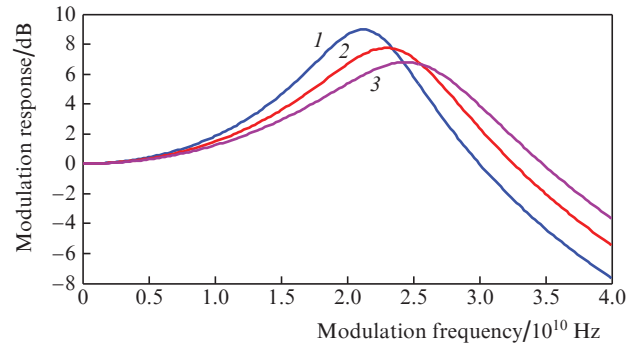


Figure 6. Modulation response at injection current densities $J =$ (1) $3J_{\text{th}}$, (2) $3.5J_{\text{th}}$ and (3) $4J_{\text{th}}$.

of TI QD lasers. In fact, with increasing tunnelling probability, the number of injected carriers into the GS increases. Figure 7 illustrates the impact of the tunnelling probability on the modulation response of a TI QD laser. For $\epsilon_t = 0.95$, we have the best modulation response and therefore a bandwidth of about 33.27 GHz.

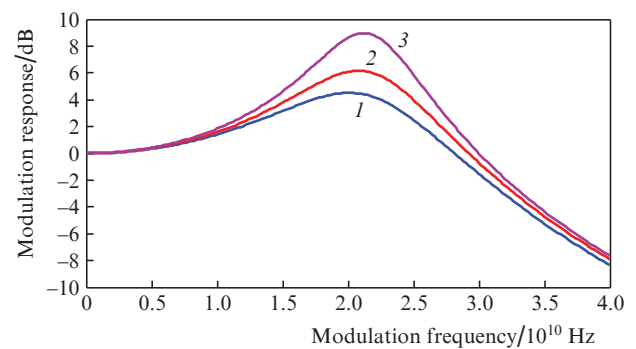


Figure 7. Modulation response at tunnelling probabilities $\epsilon_t =$ (1) 0.75, (2) 0.85 and (3) 0.95.

Figure 8 compares the modulation response of a conventional QD laser under optical feedback with that of a TI QD laser at $\epsilon_t = 0.75$. One can see that the bandwidths of a conventional QD laser and a TI QD laser under optical feedback are ~ 23.8 and ~ 29.8 GHz, respectively. Thus, under the stability conditions and in the presence of optical feedback, the

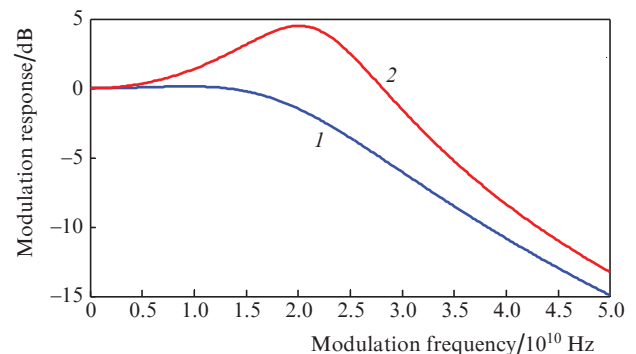


Figure 8. Comparison of modulation responses of (1) a conventional QD laser and (2) a TI QD laser.

modulation bandwidth of the TI QD laser is better than that of a conventional QD laser.

Finally, Fig. 9 shows the photon density in a TI QD laser at $J = 3J_{th}$ as a function of time for the free running case and under optical feedback with $F_{ext} = 10^{-3}$. One can see that in a TI QD laser under optical feedback, the turn-on delay time is shorter which indicates that the carrier lifetime is decreased.

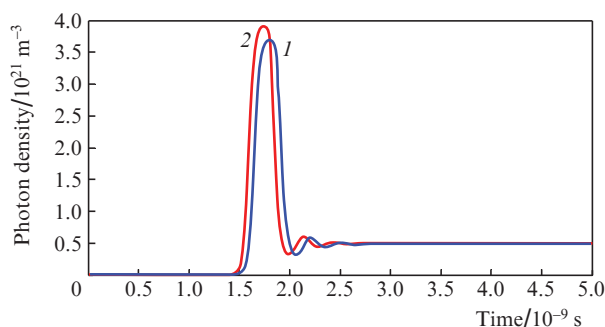


Figure 9. Time dependence of the photon density at $J = 3J_{th}$ for a TI QD laser (1) without and (2) with optical feedback at $F_{ext} = 10^{-3}$.

4. Conclusions

A new theoretical modelling has been presented to evaluate the modulation response of TI QD lasers under optical feedback through a small-signal analysis. The numerical solution of the system of rate equations for the carriers, photons and phase shows the important role of optical feedback in the formation of the modulation response of TI QD lasers. The impacts of different parameters, such as the feedback ratio, external cavity length, injection current, tunnelling probability and LEF, on the modulation response and dynamics of TI QD lasers have been investigated. The results show that the modulation bandwidth and the relaxation frequency improve under an appropriate feedback level, a short external cavity and a high tunnelling probability. Finally, the modulation response of a TI QD laser with and without feedback has been compared with that of a conventional QD laser. It is shown that under proper optical feedback, TI QD lasers would have a better bandwidth and dynamics than conventional QD lasers.

References

- Liu G., Stintz A., Li H., Malloy K., Lester L. *Electron. Lett.*, **35**, 1163 (1999).
- Zhou D., Piron R., Grillot F., Dehaese O., Homeyer E., et al. *Appl. Phys. Lett.*, **93**, 161104 (2008).
- Mikhrin S., Kovsh A., Krestnikov I., Kozhukhov A., Livshits D., Ledentsov N., et al. *Semicond. Sci. Technol.*, **20**, 340 (2005).
- Smowton P.M., Elliott S.N., Shutts S., Al-Ghamdi M.S., Krysa A.B. *IEEE J. Sel. Top. Quantum Electron.*, **17**, 1343 (2011).
- Drzewietzki L., Thè G.A., Gioannini M., Breuer S., Montrosset I., Elsässer W., et al. *Opt. Commun.*, **283**, 5092 (2010).
- Li S.G., Gong Q., Cao C.F., Wang X.Z., Chen P., Yue L., Liu Q.B., Wang H.L., Ma C.H. *Mater. Sci. Semicond. Process.*, **15**, 86 (2012).
- Kuntz M., Fiol G., Lämmlin M., Schubert C., Kovsh A., Jacob A., et al. *Electron. Lett.*, **41**, 244 (2005).
- Xu P.-F., Yang T., Ji H.-M., Cao Y.-L., Gu Y.-X., Liu Y., et al. *J. Appl. Phys.*, **107**, 013102 (2010).
- Saito H., Nishi K., Kamei A., Sugou S. *IEEE Photon. Technol. Lett.*, **12**, 1298 (2000).
- Jiao Z., Lu Z., Liu J., Poole P., Barrios P., Poitras D., et al. *Opt. Commun.*, **285**, 4372 (2012).
- Bhattacharya P., Ghosh S., Pradhan S., Singh J., Wu Z.-K., et al. *IEEE J. Quantum Electron.*, **39**, 952 (2003).
- Grillot F., Wang C., Naderi N.A., Even J. *IEEE J. Sel. Top. Quantum Electron.*, **19**, 1900812 (2013).
- Otto C., Globisch B., Lüdge K., Schöll E. *Int. J. Bifurcation Chaos*, **22**, 1250246 (2012).
- Yu Y., Xi J. *Opt. Lett.*, **38**, 1781 (2013).
- Virte M., Panajotov K., Sciamanna M. *2013 Conf. on Lasers and Electro-Optics Europe and Int. Quantum Electron. Conf. (CLEO EUROPE/IQEC)* (Munich, 2013), doi: 10.1109/CLEOE-IQEC.2013.6801840.
- Wang C., Even J., Grillot F. *IET Optoelectron.*, **8**, 51 (2014).
- Qasaimeh O., Khanfar H. *IEE Proc. Optoelectron.*, **151**, 143 (2004).
- Al-Khursan A.H., Ghalib B.A., Al-Obaidi S.J. *Semicond.*, **46**, 213 (2012).